Published in final edited form as:
Dev Dyn. 2007 July ; 236(7): 1905–1917. doi:10.1002/dvdy.21192.

Disruption of *Fibroblast Growth Factor Receptor 3* Signaling Results in Defects in Cellular Differentiation, Neuronal Patterning, and Hearing Impairment

Chandrakala Puligilla[1,*], **Feng Feng**[2], **Kotaro Ishikawa**[3], **Stefano Bertuzzi**[4], **Alain Dabdoub**[1], **Andrew J. Griffith**[3], **Bernd Fritzsch**[2], and **Matthew W. Kelley**[1]

[1]Section on Developmental Neuroscience, NIDCD/NIH, Bethesda, Maryland [2]Department of Biomedical Sciences, Creighton University, Omaha, Nebraska [3]Otolaryngology Branch, NIDCD/NIH, Rockville, Maryland [4]Mammalian Development Section, NINDS/NIH, Bethesda, Maryland

Abstract

Deletion of *fibroblast growth factor receptor 3 (Fgfr3)* leads to hearing impairment in mice due to defects in the development of the organ of Corti, the sensory epithelium of the Cochlea. To examine the role of FGFR3 in auditory development, cochleae from $Fgfr3^{-/-}$ mice were examined using anatomical and physiological methods. Deletion of *Fgfr3* leads to the absence of inner pillar cells and an increase in other cell types, suggesting that FGFR3 regulates cell fate. Defects in outer hair cell differentiation were also observed and probably represent the primary basis for hearing loss. Furthermore, innervation defects were detected consistent with changes in the fiber guidance properties of pillar cells. To elucidate the mechanisms underlying the effects of FGFR3, we examined the expression of *Bmp4*, a known target. *Bmp4* was increased in $Fgfr3^{-/-}$ cochleae, and exogenous application of bone morphogenetic protein 4 (BMP4) onto cochlear explants induced a significant increase in the outer hair cells, suggesting the Fgf and Bmp signaling act in concert to pattern the cochlea.

Keywords

hair cell; cochlea; BMP4; Prox1; innervation; Deiters' cells; Pillar cells; microtubules; stria vascularis

INTRODUCTION

Auditory perception in mammals is mediated through a sensory epithelium, known as the organ of Corti, located within the coiled cochlea in the ventral region of the inner ear. The organ of Corti is composed of two basic cell types, mechanosensory hair cells and nonsensory supporting cells. Hair cells are arranged into a single row of inner hair cells (IHCs) and three rows of outer hair cells (OHCs). IHCs are predominantly innervated by afferent fibers and are the primary auditory receptor cells. In contrast, OHCs are predominantly innervated by efferent fibers and play a mechanical role in regulating basilar membrane motion in response to incoming sound vibrations (Liberman et al., 2002). The population of supporting cells includes several highly specialized cell types, such as, inner pillar cells (IPCs), outer pillar cells (OPCs), Deiters' cells, Hensen's cells, and Claudius

[*]Correspondence to: Chandrakala Puligilla, NIDCD/NIH, Bldg 35, Room 2A-205, Convent Drive, Bethesda, MD 20892. puligillac@nidcd.nih.gov.

cells. The IPCs and OPCs combine to form the tunnel of Corti, a fluid filled triangular space that separates the single row of IHCs from the first row of OHCs (OHC1; reviewed in Lim, 1986). Pillar cells and Deiters' cells are unique to the mammalian cochlea, and although their specific function is unknown, their appearance coincides with the elongation of the cochlea and an increased range of frequency sensitivity in early mammalian ancestors (Manley, 2000), suggesting that these cell types play a role in the perception of high frequencies.

While considerable progress has been made in the identification of the molecules that specify cochlear sensory epithelia and hair cell formation (Erkman et al., 1996; Xiang et al., 1998; Bermingham et al., 1999; Wallis et al., 2003; Woods et al., 2004; Hertzano et al., 2004; Fritzsch et al., 2005a; Kiernan et al., 2005a,b), advances in the understanding of factors that regulate supporting cell development have been lacking. However, pillar cell development is affected in mice with a targeted disruption in *Fibroblast growth factor receptor 3* (*Fgfr3*; Colvin et al., 1996). Fibroblast growth factor receptor 3 (FGFR3) is a member of the Fgf signaling family that includes 22 known secreted Fgf ligands and four transmembrane receptors, numbered 1 to 4. All Fgfrs are tyrosine kinase receptors that are dependent on Fgf binding for activation (reviewed in Zhang et al., 2006).

Deletion of *Fgfr3* in mice leads to multiple defects, including significant auditory impairment as it is thought to play a role in development of pillar cells within the organ of Corti (Colvin et al., 1996; Mueller et al., 2002). The observation that FGFR3 expression within the developing organ of Corti includes not only cells that will develop as pillar cells, but also cells that will develop as OHCs and Deiters' cells (Peters et al., 1993; Mueller et al., 2002), combined with the high level of hearing impairment in these animals suggested that FGFR3 could have additional roles in cochlear development.

RESULTS

Fgfr3 Null Mice Have Increased Auditory Brain Stem Response Thresholds

Fgfr3$^{-/-}$ mutant mice showed a significant increase in auditory brain stem response (ABR) thresholds across all tested frequencies (Fig. 1A) as previously shown by Colvin et al. (1996). Threshold shifts of approximately 50 dB were observed at each tested frequency. However, in contrast with the results reported by Colvin et al., we were able to observe responses at sound intensities below 100 dB. In fact, the threshold at 32 kHz was approximately 70 dB. In addition, although overall ABR sensitivity was significantly elevated at all tested frequencies in *Fgfr3*$^{-/-}$ mice, a 20 dB downward shift was observed between 16 and 32 kHz. This shift paralleled a similar shift in wild-type (WT) mice between the same frequencies.

Number of Pillar Cells Is Reduced in *Fgfr3*$^{-/-}$ Mice

Previous results (Colvin et al., 1996) had indicated that pillar cells were present but undifferentiated in *Fgfr3*$^{-/-}$ mice. Therefore, we began our analysis by examining the pillar cell space located between IHC and OHC1. Whereas two cell nuclei were usually present in the pillar cell space in the basal turn of the cochlea, single nuclei were often present in the same region in the middle and apical turns (Fig. 2A–C). The low level of differentiation in these cells made it impossible to determine their identity based on morphology. Therefore, the identity and morphology of cells located between IHC and OHC1 in *Fgfr3*$^{-/-}$ and WT littermates was examined throughout the cochlea at birth (P0) using multiple markers for pillar cells. As a first step, the morphology of the distinctive pillar heads was examined by labeling the membrane-associated actin network with phalloidin. In WT cochlea, a row of cuboidal inner pillar heads and diamond-shaped outer pillar heads are clearly present (Fig.

3A). In contrast, in *Fgfr3*$^{-/-}$ cochleae, the luminal surfaces of cells located between IHC and OHC1 have a diamond shape that appears similar to the outer pillar heads (Fig. 3B). In addition, the diamond-shaped outer pillar heads are the only cells spanning the gap between IHC and OHC1, and, in contrast with WT, are often in contact with both IHCs and OHCs. The neurotrophin receptor p75^{ntr} has been shown to specifically label both IPCs and OPCs, and is absent in cochlear explants that have been treated with SU5402 (Mueller et al., 2002). In a WT cochlea at P0, the cuboidal inner pillar heads strongly express p75^{ntr} (Fig. 3C, arrowhead). Moreover, both the diamond-shaped outer pillar heads and the extensions of those heads that form interdigitations between the first-row OHCs are also positive for p75^{ntr} (Fig. 3E, arrowhead). In contrast, in *Fgfr3*$^{-/-}$ mutants, the expression of p75^{ntr} is markedly reduced and the row of cuboidal p75^{ntr}-positive IPCs is missing (Fig. 3D,F), suggesting that IPCs are absent in these cochleae. However, the p75^{ntr}-positive extensions of the outer pillar heads that interdigitate between OHC1 cells are still present (Fig. 3D,F, arrowheads).

Recently, the prospero-related transcription factor Prox1, has been shown to specifically label the nuclei of IPCs and OPCs and Deiters' cells (Bermingham-McDonogh et al., 2006). Therefore, the expression of this marker was also examined. In WT cochleae, Prox1-labeling at P0 clearly indicates a single row of oblong-shaped, tightly packed, IPC nuclei (Fig. 3G). Next to this distinct row of IPC nuclei are four rows of nuclei with a more rounded shape. These cells represent the single row of OPC and three rows of Deiters' cells (Fig. 3G). In contrast, in *Fgfr3*$^{-/-}$ cochleae; the number of rows of Prox1-positive cells varies between four and five (Fig. 3H). Moreover, regardless of the number of rows of Prox1-positive cells, oblong-shaped nuclei were never observed. Cryostat sections through the organ of Corti at P0 indicated the presence of a variable number of Prox1-positive cells in the space between IHC and OHC1. While two Prox1-positive cells, the IPC and OPC, were invariably present in WT (Fig. 3I), either two (Fig. 3J) or one (Fig. 3K) Prox1-positive cells were present in this space in *Fgfr3*$^{-/-}$ cochleae. These results are consistent with the observation of variable numbers of Prox1-positive cells in the pillar cell region as illustrated in Figure 3H. Because all indications of differentiated IPCs are completely missing in these mutants, and, in many cases, even the cells themselves appear to be absent, it can be suggested that FGFR3 plays a role in the commitment of cells to this phenotype.

Number of Outer Hair Cells and Deiters' Cells Is Increased in *Fgfr3*$^{-/-}$ Mice

If FGFR3 plays a role in commitment of cells to the IPC fate, then deletion of *Fgfr3* might result in some FGFR3-positive progenitors assuming an alternate cell fate. Because the initial domain of FGFR3 expression also includes cells that will develop as OHCs and Deiters' cells (Peters et al., 1993; Pirvola et al., 1995; Mueller et al., 2002), the number of each of these cells was analyzed using a combination of cell type-specific markers and cellular morphology. Analysis of IHCs and OHCs using an antibody against Myosin6 (Myo6) indicated the presence of an obliquely interlacing extra row of OHCs in *Fgfr3*$^{-/-}$ cochleae at P0 (Fig. 4A–F). Although there was some minor variability, the extra OHC row typically began at a position approximately 40% from the base of the cochlea and extended continuously for the apical 60%. Quantification of the total number of IHCs and OHCs in cochleae from WT and *Fgfr3*$^{-/-}$ littermates indicated that the number of OHCs significantly increased from an average of 1,760 in WT to 2,170 in *Fgfr3*$^{-/-}$ cochleae (Fig. 4G). In contrast, there was no change in the number of IHCs (Fig. 4G). There was no statistical difference in the length of the cochleae between WT and *Fgfr3*$^{-/-}$ mice, indicating that the change in hair cell number is not a result of an increased packing density of OHC in a shortened cochlea (data not shown) as previously reported for *Neurog1*$^{-/-}$ (Ma et al., 2000; Matei et al., 2005), *Vangl2*$^{-/-}$ (Montcouquiol et al., 2003), and *FoxG1*$^{-/-}$ mice (Pauley et al., 2006).

Hair cells have been shown to recruit surrounding cells to develop as supporting cells (Woods et al., 2004). Therefore, labeling with S100A1, a marker for Deiters' cells (Coppens et al., 2001), was used to determine whether the increased number of OHCs in *Fgfr3*$^{-/-}$ mutants resulted in an increase in the number of Deiters' cells. In contrast with the three highly ordered rows of Deiters' cells observed in WT cochleae (Fig. 4H), S100A1 labeling indicated the presence of four disorganized rows of Deiters' cells in the apical 60% of *Fgfr3*$^{-/-}$ cochleae (Fig. 4I). To determine whether changes in the number of OHCs and Deiters' cells could be accounted for by changes in the fates of cells within the FGFR3 domain, the total number of cells that derived from the *Fgfr3* expression domain (pillar cells + OHCs + Deiters' cells) in WT and *Fgfr3*$^{-/-}$ littermates were determined. Results indicated that the total number of cells within the *Fgfr3* domain significantly increased from an average of 4,784 in WT to 5,219 in *Fgfr3*$^{-/-}$ mutants (Fig. 4J). However, the number of Prox1-positive cells was unchanged, indicating that the increase in cells within the *Fgfr3* expression domain was completely attributable to the increase in OHCs. Because FGFR3 has been shown to regulate cellular proliferation in chon-drocytes (Naski et al., 1998), we examined whether the deletion of *Fgfr3* leads to an increase in proliferation within the cochlea by incorporation of bromodeoxyuridine (BrdU). No change in the level of proliferation within the cochlea was observed between WT and *Fgfr3*$^{-/-}$ littermates (data not shown). Similarly, no change in the level of cell death was observed (data not shown). These data suggest that altered cell fate rather than additional proliferation is the basis for the cellular increase in the organ of Corti. Moreover, the overall increase in cell number suggests that loss of *Fgfr3* probably leads to recruitment of cells from outside the *Fgfr3* domain.

Differentiation of Outer Hair Cells and Deiters' Cells Is Altered in *Fgfr3*$^{-/-}$ Mice

In addition to pillar cells, FGFR3 is initially expressed in cells that will develop as OHCs and Deiter's cells. Because the differentiation of IPCs is affected in *Fgfr3*$^{-/-}$ mutants, we wanted to determine whether the differentiation of other FGFR3-positive cells would also be affected. To examine an effect on OHC function, expression of Prestin, an OHC-specific protein, was examined. While Prestin is expressed in OHCs in *Fgfr3*$^{-/-}$ cochleae, the overall level appears to be reduced by comparison with WT (Fig. 5A,B), suggesting a defect in the OHC function. To further examine any potential defects in OHC differentiation, distortion product otoacoustic emissions (DPOAEs) were measured. While WT DPOAEs showed amplitudes of 20 to 40 dB above the noise floor (background) at f2 frequencies between 10 and 20 kHz, DPOAEs for *Fgfr3*$^{-/-}$ mutants did not differ significantly from the noise floor at any of the test frequencies (Fig. 1B). To confirm that defects in DPOAE were not a result of defects in development of the middle ear bones or of chronic otitis media, a morphological analysis of the middle ear space was conducted. No otitis media or defects in middle ear bones were observed in WT or *Fgfr3*$^{-/-}$ littermates (data not shown), suggesting a defect in OHC function.

S100A1-labeling of Deiters' cells in *Fgfr3*$^{-/-}$ mutants indicated defects in organization and patterning. Based on these observations, it seemed likely that FGFR3 might play a role in differentiation of Deiters' cells as well. To examine the role of FGFR3 in these events, developing microtubule bundles in pillar cells and Deiters' cells were labeled with anti–β-tubulin I + II antibodies at P0. In WT cochleae, microtubules in IPCs develop as bundles that extend from the basal region of the cell to the luminal surface. At the luminal surface, the terminations of these bundles within each IPC appear as a row of rectangular-shaped structures (Fig. 5C,E). In contrast with IPCs, in OPCs and first and second-row Deiters' cells (D1,D2), microtubule bundles extend laterally beneath the luminal surface of each cell to form interdigitations between the three rows of OHCs (Fig. 5C,E). Within each row, microtubule bundles are arranged into a characteristic morphology that is present in all cells

within that row. Finally, third-row Deiters' cells do not form interdigitations and instead create a border at the outer edge of the organ of Corti.

In comparison with WT, pillar cell and Deiters' cell patterning was markedly disrupted in *Fgfr3*$^{-/-}$ cochleae (Fig. 5D,F). In particular, the rectangular row of IPCs was completely absent throughout the mid-base and the apical part of the cochlea. The ordered rows of Deiters' cells were disrupted, and many cells extended aberrant interdigitations. For instance, in some cases, Deiters' cell microtubule bundles were observed to project toward the medial edge of the epithelium to form inappropriate interdigitations between OHCs (Fig. 5D, shown in arrows). In other cases, individual Deiters' cells were observed to project microtubule bundles toward both the lateral and medial edges of the epithelium. Also in rare cases, a Deiters' cell was observed to form interdigitations on both sides of a single OHC. Finally, third-row Deiters' cells, which do not extend interdigitations in WT, were observed to generate interdigitations that projected toward the medial side of the organ of Corti to separate third-row OHCs (Fig. 5D, shown in arrowheads).

Innervation Is Disrupted in *Fgfr3*$^{-/-}$ Cochleae

It has been suggested that pillar cells may play a role in regulating the patterning of innervation in the organ of Corti (Ginzberg and Morest, 1983; Sobkowicz and Emmerling, 1989). Therefore, because pillar cell development is disrupted in *Fgfr3*$^{-/-}$ cochleae, it seemed possible that defects in innervation could be an underlying contributor to the overall level of auditory dysfunction. As a first step, afferent and efferent nerve fibers were visualized by labeling with an anti-Neurofilament antibody at P8. In WT, the majority of fibers terminate on the IHCs with the remainder of the fibers crossing the tunnel of Corti and then turning toward the base of the cochlea to form three rows of spiral fibers (Fig. 6A). In *Fgfr3*$^{-/-}$ cochleae, increased numbers of apparently disorganized fibers crossed the tunnel (Fig. 6B). In particular, discrete bundles of spiral fibers were not obvious and there was a marked increase in the number of crossing fibers. Because Neurofilament is expressed in both afferent and efferent fibers, we next examined afferent innervation specifically by labeling afferent fibers through injections of lipophilic dye into dorsal cochlear nucleus. Results indicated similar defects in both the number of fibers crossing the tunnel of Corti and in the organization of the spiral fibers in *Fgfr3*$^{-/-}$ mutants. However, a gradient of effects was apparent with organization in the base of the cochlea appearing comparable between WT and *Fgfr3*$^{-/-}$ (Fig. 6C,D). Afferent fiber patterns in the mid-base were consistent with the results obtained with Neurofilament staining in the same region (Fig. 6A,B), including increased numbers of crossing fibers and disruption of spiral fiber bundles in the *Fgfr3*$^{-/-}$ (Fig. 6E,F). At P1, spiral fibers are not fully organized in the apex (Fig. 6G); however, an increase in the number of crossing fibers and an obvious disorganization was apparent in the *Fgfr3*$^{-/-}$ mutant (Fig. 6H).

To determine whether the changes in fiber formation could be correlated with differences in supporting cell patterning, we compared fiber morphology with the position of hair cell and supporting cell nuclei in the unaffected base and affected mid-basal regions of an *Fgfr3*$^{-/-}$ cochleae at P1. In the unaffected base, fibers project laterally from the IHC region across the pillar cell space before turning beneath one of the rows of OHCs (Fig. 6I,J). At the level of the supporting cell nuclei, fibers do not turn until they reach the lateral edge of the second row of pillar cells. In contrast, in the affected mid-base, the distance between IHCs and first-row OHCs is noticeably reduced. As a result, fibers begin to turn almost as soon as they extend beyond the IHCs (Fig. 6L,M). Spiral fibers are still aligned along rows of supporting cell nuclei, but the relatively poor organization of these rows appears to contribute to the disorganization of the spiral fibers (Fig. 6N).

FGFR3 Acts as a Negative Regulator of *Bmp4*

The results described above suggested a role for FGFR3 in regulating cell fate choice within the organ of Corti and, in particular, in the determination of whether progenitor cells would develop as pillar cells or OHCs. To identify the signaling pathways that might mediate these effects, downstream targets of FGFR3 signaling were examined. Previous results have demonstrated multiple examples of interactions between the Fgf and Bmp signaling pathways (reviewed in Massague et al., 2005) and in particular between FGFR3 and bone morphogenetic protein 4 (BMP4; Naski et al., 1998). Therefore, levels of mRNA for *Bmp4* in cochleae from WT and *Fgfr3*$^{-/-}$ mutants were determined at embryonic day (E) 15.5 and P0 by semiquantitative polymerase chain reaction (PCR; Fig. 7A,B). Results indicated an increase in the mRNA levels of *Bmp4* in *Fgfr3*$^{-/-}$ cochleae as compared with WT, suggesting that *Fgfr3* also acts to negatively regulate *Bmp4* in the cochlea.

Previous studies have demonstrated that *Bmp4* is not expressed in hair cells, pillar cells, or Deiters' cells within the organ of Corti, but is expressed in Hensen's cells and Claudius cells, which are located directly lateral to the third row of Deiters' cells (Morsli et al., 1998). To examine the role of *Bmp4* in the organ of Corti, cochlear explants were exposed to different concentrations of Noggin, a BMP4 (as well as, BMP2 and BMP7) antagonist, beginning on E15.5. Changes in development of the organ of Corti were determined by labeling hair cells with the Myob antibody and by labeling cell boundaries with phalloidin. The timing of addition of Noggin was based on the onset of expression for *Fgfr3*. Exposure to Noggin led to a dose-dependent decrease in the number of OHCs but appeared to have no effect on IHCs (Fig. 7C,D, and data not shown). To determine whether increased levels of BMP4 could account for the increased number of hair cells observed in *Fgfr3*$^{-/-}$ cochleae, heparin–acrylic beads soaked in BMP4 (40 μg/ml) were inserted into the sensory epithelium of cochlear explants at E15.5. The presence of BMP4-soaked beads induced the formation of extra OHCs but had no effect on the number of IHCs (Fig. 7E–H). The effects of BMP4-soaked beads were limited to regions of the epithelium located within 200 μm of the bead (Fig. 7F,H), suggesting that a relatively high concentration of BMP4 is required to influence hair cell formation. In contrast, control beads soaked in saline had no effect on OHC number (Fig. 7E,G). The effects of both Noggin treatment and BMP4-soaked beads were significant (Fig. 7K). In contrast with its effects on hair cells, the number and location of pillar cells appeared normal in the presence of BMP4-soaked beads (Fig. 7F,H, and data not shown).

Finally, to determine whether FGFR3 and BMP4 influence hair cell development through the same signaling pathway, cochlear explants were established from *Fgfr3*$^{-/-}$ mutants at E13.0 and exposed to Noggin (3 μg/ml) beginning on E15.5. Untreated *Fgfr3*$^{-/-}$ explants developed between one and three extra rows of OHCs in addition to the normal three rows of OHCs (Fig. 7I). In contrast, treatment of *Fgfr3*$^{-/-}$ explants with Noggin reduced the number of OHCs to approximately three rows (Fig. 7J). Quantification of the density of OHCs in *Fgfr3*$^{-/-}$ untreated and *Fgfr3*$^{-/-}$ Noggin-treated explants indicated that the increase in the density of OHCs in *Fgfr3*$^{-/-}$ explants was reduced to levels that were comparable to WT in *Fgfr3*$^{-/-}$ explants that were exposed to Noggin (Fig. 7K). IHCs appeared unaffected in both *Fgfr3*$^{-/-}$ and *Fgfr3*$^{-/-}$ + Noggin treatments, and pillar cells were absent in both conditions.

DISCUSSION

Inner Pillar Cells Are Absent in *Fgfr3*$^{-/-}$ Mice

In their original description of the cochlear phenotype in *Fgfr3*$^{-/-}$ mice, Colvin et al. (1996) noted that pillar cells were present, but undifferentiated. However, because makers for pillar cells or other cell types within the organ of Corti had not been identified at that time, this

conclusion was based solely on morphological characteristics. In contrast, the results presented here strongly suggest that, whereas OPCs are present but undifferentiated, IPCs are missing. First, in many cases, only a single cell is located in the space between the row of IHCs and the first row of OHCs. Second, the row of cuboidal IPC heads that normally separate IHCs and first-row OHCs is missing, as are the microtubule bundles that are normally located in those cells. Moreover, no cells with oblong nuclei, a distinctive trait of IPCs, are present in the organ of Corti in *Fgfr3*$^{-/-}$ mutants. Finally, the expression of two markers of pillar cells, p75^{ntr} and Prox1 are both absent from the region between IHCs and first-row OHCs. However, it is important to note that both markers are still expressed in cells that extend interdigitations between first-row OHCs, suggesting that OPCs are present. Similar results for the expression p75^{ntr} and Prox1 in *Fgfr3*$^{-/-}$ mutants were recently reported (Hayashi et al., 2007).

The absence of IPCs in *Fgfr3*$^{-/-}$ cochleae suggests that FGFR3 signaling plays a role in the determination of IPC fate. This hypothesis is supported by the increased number of OHCs and Deiters' cells, in the absence of increased proliferation, in *Fgfr3*$^{-/-}$ cochleae, suggesting that cells that would have developed as IPC have switched fates to develop as additional hair cells and Deiters' cells. Consistent with this interpretation, deletion of *Sprouty2*, an Fgfr antagonist, leads to an increase in the number of pillar cells (Shim et al., 2005).

A similar increase in the number of OHCs in *Fgfr3*$^{-/-}$ mice has recently been reported by Hayashi et al. (2007) but was not reported in the initial description of the *Fgfr3*$^{-/-}$ phenotype (Colvin et al., 1996). The reasons for this difference are not clear, but could be related to background strain or method of analysis. Animals were maintained on a C57Bl/6 background, the same strain used in Colvin et al. (1996), but the quantity of hair cells in that study are presented as density rather than total number per cochleae. The change in hair cell number, while significant, is limited to a single extra row of hair cells, and is not present along the entire length of the cochlea. Therefore, it seems possible that the method of analysis used in Colvin et al. might not have revealed the change. In fact, a slight increase in OHC density is reported in Colvin et al. (1996) and one of the images presented includes a single extra row of hair cells.

As discussed above, based on morphological data and expression of cell-specific markers, IPCs appear to be absent in *Fgfr3*$^{-/-}$ cochleae, leading to the nearly direct apposition of IHCs and first-row OHCs. However, an equally valid alternate hypothesis would be that, while inner pillar differentiation is disrupted in *Fgfr3*$^{-/-}$ mutants, the IPCs themselves are still present and that the effect of loss of FGFR3 signaling is to allow an additional row of OHCs to form in the region between the IPCs and OPCs. The organ of Corti is composed of a largely invariant mosaic in which each supporting cell is separated from each neighboring supporting cell by a single hair cell. However, this mosaic is disrupted by the homogenous row of IPCs. One possible mechanism for the development of this row would be the active inhibition of hair cell formation in this region. In *Fgfr3*$^{-/-}$ mice, the total number of OHCs is increased and the alternating mosaic of hair cells and supporting cells is largely intact (Fig. 2A,B). This finding could be a result of the formation of an additional row of OHCs in between the cells that would normally develop as IPCs. Unfortunately, the disruption in the morphological development of supporting cell types makes it impossible to determine whether the extra row of OHCs is located between the cells that would have developed as IPCs or at the more lateral edge of the organ of Corti. However, the hypothesis that FGFR3 signaling plays a role in inhibition of hair cell formation is supported by the demonstration that increased activation of FGFR3 in vitro leads to an inhibition in hair cell formation (Jacques et al., personal communication).

FGFR3 Regulates Cellular Differentiation in the Organ of Corti

In addition to the absence of IPCs, significant disruptions in the differentiation of OPCs, OHCs, and Deiters' cells were also observed in *Fgfr3*$^{-/-}$ cochleae. The characteristic cellular patterning of both OPCs and Deiters' cells were clearly disrupted, as were the microtubule bundles within both cell types. In addition, expression of the OHC motor protein Prestin was markedly decreased in OHCs in *Fgfr3*$^{-/-}$ cochleae and otoacoustic emissions were absent, indicating defects in OHC function. The cell types affected in these cochleae, OPCs, OHCs, and Deiters' cells correlate with the population of progenitor cells that express *FGFR3* between E16 and P0. Based on this observation, it seems possible that FGFR3 could play a direct role in regulating the differentiation of each of these cell types. However, it is also possible that the differentiation defects are a secondary result of a more limited effect of deletion of *Fgfr3*. For instance, hair cells are known to generate inductive signals that modulate the fate and differentiation of surrounding cells (Lanford et al., 1999; Woods et al., 2004; Kiernan et al., 2005); therefore, it seems possible that the presence of IPCs might be required for subsequent differentiation of other cell types within the organ of Corti. Additional experiments in which *Fgfr3* is deleted in specific subsets of cells within the organ of Corti are clearly required to address these hypotheses.

FGFR3/BMP4 Interactions Regulate the Number of Outer Hair Cells

As discussed, deletion of *Fgfr3* leads to an increase in the number of OHCs and to an increase in the expression of mRNA for *Bmp4*. Modulation of BMP4 signaling either with Noggin or BMP4 protein directly affects the number of OHCs, with BMP4 acting as an inducer of OHC formation. In addition, treatment of *Fgfr3*$^{-/-}$ explants with Noggin was sufficient to return the number of OHC to normal, suggesting the BMP signaling mediates the effects of FGFR3 on OHC development. However, it is also possible that BMP4 and Fgfr3 act through parallel pathways that both independently influence OHC formation. Further experiments are clearly required to discriminate between these two possibilities. The effects of modulation of BMP signaling observed here are consistent with recently published work using chick otocysts in which treatment with BMP4 acted to increase the number of cells that developed as hair cells (Li et al., 2005). However, it should also be noted that a second study found the exact opposite result, with Noggin treatment increasing the number of hair cells while BMP4 acted to inhibit hair cell formation (Pujades et al., 2006).

During cochlear development, *Bmp4* is expressed in cells located lateral to the developing OHC domain (Morsli et al., 1998). While it has not been specifically examined, the region of *Bmp4* expression appears to either overlap slightly with the lateral edge of the *Fgfr3* expression domain, or, more likely, to be located directly adjacent to it (Morsli et al., 1998), suggesting that FGFR3 signaling, either directly or indirectly, acts to inhibit the expression of BMP4 in this lateral domain and, therefore, to regulate the number of cells that develop as OHCs. This signaling interaction could play a role in patterning the OHC domain. With the exception of the organ of Corti and the saccular and utricular macula, BMP4 is expressed in all developing hair cell sensory epithelia in birds and mammals (Oh et al., 1996; Cole et al., 2000). The basis for the lateral shift in *Bmp4* expression in the cochlea is not clear, but could be a result of the unique expression of *Fgf8* in IHCs (Pirvola et al., 2002; Shim et al., 2005). It has been proposed that BMP4 and FGF8 may actively antagonize one another during the formation of signaling centers in both the brain and limb (Ohkubo et al., 2002). And an inner ear-specific deletion of *Fgf8* phenocopies the pillar cell defect observed in *Fgfr3*$^{-/-}$ mutants (Jacques et al., personal communication), strongly suggesting that FGF8 acts as the main ligand for FGFR3 in the cochlea. However, the effects of these signaling pathways are ultimately regulated at the receptor level through activation of Fgfrs and Bmprs, and associated downstream targets, such as Smads (Massague et al., 2005). Unfortunately, the patterns of expression for Bmprs and Smads within the cochlea have not been determined,

but the data presented here would suggest that both may be expressed in developing OHCs. Based on these results, it seems possible that the pillar cell/OHC domain could be patterning through reciprocal signaling interactions between FGF8 located on its medial side and BMP4 located on the lateral side, both of which would act through activation of *FGFR3* and *BMPRS* in the progenitor domain.

Innervation Defects: Direct Effect of *Fgfr3* or Secondary Result of Pillar Cell Defects?

In *Fgfr3*$^{-/-}$ cochlea, an increased number of fibers crossed the pillar cell space to form contacts with OHCs and the overall organization of the fiber bundles was disrupted. These results are consistent with the possibility that pillar cells form a boundary that regulates the passage of only a subset of spiral ganglion neurites. Normally, only approximately 5% of all spiral ganglion neurons, the smaller, type II neurites cross the tunnel of Corti to synapse on OHCs (reviewed in Rubel and Fritzsch, 2002). At present, it is not clear whether the neurites of type II neurons are uniquely able to cross the tunnel or if it is the crossing of the tunnel that leads to these cells developing as type II neurons. Previous studies have demonstrated an important role for supporting cells, including pillar cells, in fiber guidance. For instance, deletion of the tyrosine kinase receptor *ErbB2*, which is expressed in pillar cells (Hume et al., 2003) results in defects in afferent neuronal growth with many fibers failing to enter the organ of Corti at all, and instead projecting to the lateral wall of the cochlea (Morris et al., 2006). Similarly, deletion of Neurotrophin-3 (Nt-3), which is largely expressed in supporting cells by P0, also leads to innervation defects, but, because the absence of Nt-3 leads to the death of nearly 90% of all afferent neurons by E15.5, it is difficult to separate the effects of this molecule in neuronal patterning versus survival (Farinas et al., 2001). However, considering the existing data, and, in addition, the position of the pillar cells and the fact that they express several molecules that have been shown to influence neurite outgrowth, including p75^{ntr} (reviewed in Gentry et al., 2004; Hasegawa et al., 2004) and ErbB2 (Morris et al., 2006), it seems likely that they could play a role in mediating the number of neurites that cross the tunnel. Because pillar cells are significantly disrupted throughout most of the length of the cochlea in *Fgfr3*$^{-/-}$ mice, the loss of these cells may result in a reduction or loss of inhibitory signals that normally prevent most spiral ganglion neurites from crossing the tunnel. Similarly, the observed defects in fiber fasciculation could be a result of defects in OHC development. Consistent with the finding that pillar cells are less disrupted in the base compared with mid-base and apex, we found normal crossing of fibers in the base, suggesting that crossing of neurites correlates with the degree of disruption of pillar cell patterning.

CONCLUSIONS

The results presented here expand our understanding of the roles of FGFR3 in cochlear development as well as providing a potential basis for both the functional and phenotypic consequences of loss of FGFR3. The decrease in Prestin expression and lack of otoacoustic emissions may account for the majority of the hearing loss in these mutants, as similar changes in auditory sensitivity were observed in mice with a targeted deletion in *Prestin* (Liberman et al., 2002). At a molecular level, interactions between Fgf and BMP signaling pathways apparently act to partition the lateral region of the developing organ of Corti into pillar cell and OHC domains. The boundaries between these domains appear to be somewhat plastic in that changes in the relative levels of activation of either pathway result in changes in the relative size of either domain. Future experiments examining the interplay between these two pathways should lead to a greater understanding of the specific signaling interactions that mediate the formation of this portion of the organ of Corti.

EXPERIMENTAL PROCEDURES

Generation of *Fgfr3*$^{-/-}$ Mutant Mice and Genotyping

Fgfr3$^{+/-}$ mice were kindly provided by Dr. David Ornitz (Washington University, St. Louis, MO). Mice were maintained on a mixed C57Bl/129 background and intercrossed to generate *Fgfr3*$^{-/-}$ animals. All genotypes were confirmed as previously described (Colvin et al., 1996).

ABRs and DPOAEs analyses—ABRs were measured as described (Noguchi et al., 2006) with the following modifications: when no wave forms were detectable in response to the highest stimulus intensity level of 120 dB sound pressure level (SPL) for the click, 8 or 16 kHz tone burst stimuli, the threshold was considered to be 125 dB SPL. Similarly, the threshold was considered to be 105 dB SPL when there was no detectable response to the highest intensity stimulus of 100 dB SPL for the 32-kHz tone burst. DPOAEs were recorded as previously described (Noguchi et al., 2006).

Immunohistochemistry—Cochleae were dissected from wild-type and *Fgfr3*$^{-/-}$ littermates and processed as either whole-mounts or sections. Whole-mount staining of the cochlea was performed as described in Woods et al. (2004). The following primary antibodies were used: anti-Myosin6 (Sigma, 1:200); anti-Prestin (a gift from Dr. I. Belyantseva and Dr. T. Friedman, 1:400), anti-p75^{ntr} (Chemicon, 1:1,000); anti–β-tubulin I + II (Sigma, 1:200); anti-Prox1 (Covance, 1:2,000), anti-S100A1 (DAKO, 1:100), and anti-Neurofilament-200 (Sigma, 1:200). Primary antibody binding was detected using Alexa 546-conjugated or Alexa 488-conjugated secondary antibodies (Invitrogen, 1:1,000). Filamentous actin was detected by labeling with Alexa 488-conjugated phalloidin (Invitrogen, 1:100), and nuclei were labeled with Hoechst (Sigma, 1:5). For tubulin staining, *Fgfr3*$^{-/-}$ and wild-type littermate control mice were perfused with 4% paraformaldehyde (PFA). Cochleae were dissected and incubated in primary antibody against acetylated tubulin (Sigma, 1:500) followed by an Alexa 546-conjugated secondary antibody.

Isolation of RNA and first-strand cDNA synthesis—Both wild-type and *Fgfr3*$^{-/-}$ cochleae were dissected and total RNA was isolated using Trizol (Invitrogen) reagent. The reverse transcription reaction was performed using the Superscript First strand synthesis kit (Invitrogen) from 1 μg of template RNA.

Semiquantitative PCR—PCR was performed using PCR beads (Amersham Biosciences, Little Chalfont, UK), 200 ng of cDNA, and 50 pmol sense and antisense primers for each gene of interest. The sequences of primers for *Bmp4* were as follows: Sense, 5′-GATTGGCTCCCAAGAATCAT-3′ and antisense, 5′-CCTAGCAGGACTTGGCATAA -3′; for *Ihh*: sense, 5′-TGAGAGCCTTCCAGGTCATC-3′ and antisense, 5′-CATGCCAAGCTGTGAAAGAG-3′. The amplification was performed using the following PCR conditions: 1 cycle for 2 min at 94ºC, followed by 30 cycles at 94ºC for 20 sec, 60ºC for 30 sec, and 72ºC for 30 sec followed by a final extension time of 10 min at 72ºC. The expected product sizes were 150 bp for *Bmp4*, 230 bp for *Ihh*, and 417 bp for *GAPDH* (control). PCR products generated using cDNA from either WT or *Fgfr3*$^{-/-}$ cochleae were resolved on the same 2% agarose gel. The relative quantity of each PCR product was determined by quantification of ethidium bromide intercalation. Briefly, the entire gel image was digitized and Adobe Photoshop was used to compare the average intensity (luminosity) for each set of PCR products between WT and *Fgfr3*$^{-/-}$. Care was taken to ensure that no region of the scanned image had reached saturation and a rectangle of set dimensions was used to outline each band to ensure a uniform comparison.

Cochlear explant cultures—Cochlear explants were established from ICR or *Fgfr3*$^{-/-}$mouse embryos at E13 as described in Woods et al. (2004). After 2.5 days in vitro, explants were treated with either heparin–acrylic beads (Sigma) soaked in recombinant BMP4 protein (40 μg/ml; R & D Systems) or with Noggin (5 μg/ml; R & D Systems). After 4 days, in vitro explants were fixed in 4% PFA for 30 min and processed for immunohistochemistry.

Cell proliferation—To examine cell proliferation, pregnant female mice were injected with BrdU solution (10 mg/ml in phosphate buffered saline, 50 μg/gram of body weight), three times at 3-hr intervals between E14.5 and E17. Animals were killed, and heads were fixed and embedded for cryostat sectioning.

In situ hybridization—Cochleae were dissected from embryos at different stages and fixed in 4% PFA and cryostat sectioned at a thickness of 12 μm. Sections were then processed for in situ hybridization as described previously (Morsli et al., 1998).

Plastic sectioning—Individual cochleae at different stages were dissected and fixed in 3% glutaraldehyde and 2% paraformaldehyde overnight at 4ºC. After fixation, samples were dehydrated, embedded in immuno-bed solution, sectioned at a thickness of 3 μm, and stained with thionin (Woods et al., 2004).

Labeling of afferent nerve fibers—Genotyped animals were coded and cochlear afferents were labeled by injecting NeuroVue Maroon or NeuroVue Red into the dorsal cochlear nucleus (Fritzsch et al., 2005). After sufficient diffusion time, as determined previously (Maklad and Fritzsch, 2003), ears were dissected, mounted flat on slides using a cover-slip, and viewed with a confocal microscope (Zeiss LSM 510 META laser confocal scanning system). Data were documented, and phenotypic results were then compared against the genotype.

Acknowledgments

Grant sponsor: National Institute on Deafness and Other Communication; Grant sponsor: United States–Israel Binational Science Foundation; Grant number 2003335; Grant sponsor: NIH; Grant number: RO1 DC005590.

The authors thank Chad Woods and Christopher Kramer for technical assistance and Dr. Norio Yamamoto for reading an earlier version of the manuscript. M.W.K. and A.J.G. were funded by the National Institute on Deafness and Other Communication Disorders, M.W.K. was funded by the United States–Israel Binational Science Foundation, and B.F. was funded by the NIH.

References

Bermingham NA, Hassan BA, Price SD, Vollrath MA, Ben-Arie N, Eatock RA, Bellen HJ, Lysakowski A, Zoghbi HY. Math1: an essential gene for the generation of inner ear hair cells. Science. 1999; 284:1837–1841. [PubMed: 10364557]

Bermingham-McDonogh O, Obesterle EC, Stone JS, Hume CR, Huynh HM, Hayashi T. Expression of Prox1 during mouse cochlear development. J Comp Neurol. 2006; 496:172–186. [PubMed: 16538679]

Cole LK, Le Roux I, Nunes F, Laufer E, Lewis J, Wu DK. Sensory organ generation in the chicken inner ear: contributions of bone morphogenetic protein 4, serrate1, and lunatic fringe. J Comp Neurol. 2000; 424:509–520. [PubMed: 10906716]

Colvin JS, Bohne BA, Harding GW, McEwen DG, Ornitz DM. Skeletal overgrowth and deafness in mice lacking fibroblast growth factor receptor 3. Nat Genet. 1996; 12:390–397. [PubMed: 8630492]

Coppens AG, Kiss R, Heizmann CW, Schafer BW, Poncelet L. Immunolocalization of the calcium binding S100A1, S100A5, S100A6 proteins in the dog cochlea during postnatal development. Brain Res Dev Brain Res. 2001; 126:191–199.

Erkman L, McEvilly RJ, Luo L, Ryan AK, Hooshmand F, O'Connell SM, Keithley EM, Rapaport DH, Ryan AF, Rosenfeld MG. Role of transcription factors Brn-3.1 and Brn-3.2 in auditory and visual system development. Nature. 1996; 381:603–606. [PubMed: 8637595]

Farinas I, Jones KR, Tessarollo L, Vigers AJ, Huang E, Kirstein M, de Caprona DC, Coppola V, Backus C, Reichardt LF, Fritzsch B. Spatial shaping of cochlear innervation by temporally regulated neurotrophin expression. J Neurosci. 2001; 21:6170–6180. [PubMed: 11487640]

Fritzsch B, Matei VA, Nichols DH, Bermingham N, Jones K, Beisel KW, Wang VY. Atoh1 null mice show directed afferent fiber growth to undifferentiated ear sensory epithelia followed by incomplete fiber retention. Dev Dyn. 2005a; 233:570–583. [PubMed: 15844198]

Fritzsch B, Muirhead KA, Feng F, Gray BD, Ohlsson-Wilhelm BM. Diffusion and imaging properties of three new lipophilic tracers, NeuroVue Maroon, NeuroVue Red and NeuroVue Green and their use for double and triple labeling of neuronal profile. Brain Res Bull. 2005b; 66:249–258. [PubMed: 16023922]

Gentry JJ, Barker PA, Carter BD. The p75 neurotrophin receptor: multiple interactors and numerous functions. Prog Brain Res. 2004; 146:25–39. [PubMed: 14699954]

Ginzberg RD, Morest DK. A study of cochlear innervation in the young cat with the Golgi method. Hear Res. 1983; 10:227–246. [PubMed: 6863156]

Hasegawa Y, Yamagishi S, Fujitani M, Yamashita T. p75 neurotrophin receptor signaling in the nervous system. Biotechnol Annu Rev. 2004; 10:123–149. [PubMed: 15504705]

Hayashi T, Cunningham D, Bermingham-McDonogh O. Loss of Fgfr3 leads to excess hair cell development in the mouse organ of Corti. Dev Dyn. 2007; 236:525–533. [PubMed: 17117437]

Hertzano R, Montcouquiol M, Rashi-Elkeles S, Elkon R, Yucel R, Frankel WN, Rechavi G, Moroy T, Friedman TB, Kelley MW, Avraham KB. Transcription profiling of inner ears from Pou4f3(ddl/ddl) identifies Gfi1 as a target of the Pou4f3 deafness gene. Hum Mol Genet. 2004; 13:2143–2153. [PubMed: 15254021]

Hume CR, Kirkegaard M, Oesterle EC. ErbB expression: the mouse inner ear and maturation of the mitogenic response to heregulin. J Assoc Res Otolaryngol. 2003; 4:422–443. [PubMed: 14690060]

Kiernan AE, Cordes R, Kopan R, Gossler A, Gridley T. The Notch ligands DLL1 and JAG2 act synergistically to regulate hair cell development in the mammalian inner ear. Development. 2005a; 132:4353–4362. [PubMed: 16141228]

Kiernan AE, Pelling AL, Leung KK, Tang AS, Bell DM, Tease C, Lovell-Badge R, Steel KP, Cheah KS. Sox2 is required for sensory organ development in the mammalian inner ear. Nature. 2005b; 434:1031–1035. [PubMed: 15846349]

Lanford PJ, Lan Y, Jiang R, Lindsell C, Weinmaster G, Gridley T, Kelley MW. Notch signaling pathway mediates hair cell development in mammalian cochlea. Nat Genet. 1999; 21:289–292. [PubMed: 10080181]

Li H, Corrales CE, Wang Z, Zhao Y, Wang Y, Liu H, Heller S. BMP4 signaling is involved in the generation of inner ear sensory epithelia. BMC Dev Biol. 2005; 17:5–16.

Liberman MC, Gao J, He DZ, Wu X, Jia S, Zuo J. Prestin is required for electromotility of the outer hair cell and for the cochlear amplifier. Nature. 2002; 419:300–304. [PubMed: 12239568]

Lim DJ. Functional structure of the organ of Corti. Hear Res. 1986; 22:117–146. [PubMed: 3525482]

Ma Q, Anderson DJ, Fritzsch B. Neurogenin 1 null mutant ears develop fewer, morphologically normal hair cells in smaller sensory epithelia devoid of in nervation. J Assoc Res Otolaryngol. 2000; 1:129–143. [PubMed: 11545141]

Maklad A, Fritzsch B. Partial segregation of posterior crista and saccular fibers to the nodulus and uvula of the cerebellum in mice, and its development. Brain Res Dev Brain Res. 2003; 140:223–236.

Manley GA. Cochlear mechanisms from a phylogenetic viewpoint. Proc Natl Acad Sci U S A. 2000; 97:11736–11743. [PubMed: 11050203]

Massague J, Seoane J, Wotton D. Smad transcription factors. Genes Dev. 2005; 19:2783–2810. [PubMed: 16322555]

Matei V, Pauley S, Kaing S, Rowitch D, Beisel KW, Morris K, Feng F, Jones K, Lee J, Fritzsch B. Smaller inner ear sensory epithelia in Neurog 1 null mice are related to earlier hair cell cycle exit. Dev Dyn. 2005; 234:633–650. [PubMed: 16145671]

Montcouquiol M, Rachel RA, Lanford PJ, Copeland NG, Jenkins NA, Kelley MW. Identification of Vangl2 and Scrb1 as planar polarity genes in mammals. Nature. 2003; 423:173–177. [PubMed: 12724779]

Morris JK, Maklad A, Hansen LA, Feng F, Sorensen C, Lee KF, Macklin WB, Fritzsch B. A disorganized innervation of the inner ear persists in the absence of ErbB2. Brain Res. 2006; 1091:186–199. [PubMed: 16630588]

Morsli H, Choo D, Ryan A, Johnson R, Wu DK. Development of the mouse inner ear and origin of its sensory organs. J Neurosci. 1998; 18:3327–3335. [PubMed: 9547240]

Mueller KL, Jacques BE, Kelley MW. Fibroblast growth factor signaling regulates pillar cell development in the organ of Corti. J Neurosci. 2002; 22:9368–9377. [PubMed: 12417662]

Naski MC, Colvin JS, Coffin JD, Ornitz DM. Repression of hedgehog signaling and BMP4 expression in growth plate cartilage by fibroblast growth factor receptor 3. Development. 1998; 125:4977–4988. [PubMed: 9811582]

Noguchi Y, Kurima K, Makishima T, Hrabe de Angelis M, Fuchs H, Frolenkov G, Kitamura K, Griffith A. Multiple quantitative trait loci modify cochlear hair cell degeneration in the Beethoven (Tmc1Bth) mouse model of progressive hearing loss DFNA36. Genetics. 2006; 173:2111–2119. [PubMed: 16648588]

Oh SH, Johnson R, Wu DK. Differential expression of bone morphogenetic proteins in the developing vestibular and auditory sensory organs. J Neurosci. 1996; 16:6463–6475. [PubMed: 8815925]

Ohkubo Y, Chiang C, Rubenstein JL. Coordinate regulation and synergistic actions of BMP4, SHH and FGF8 in the rostral prosencephalon regulate morphogenesis of the telencephalic and optic vesicles. Neuroscience. 2002; 111:1–17. [PubMed: 11955708]

Pauley S, Lai E, Fritzsch B. Foxg1 is required for morphogenesis and histogenesis of the mammalian inner ear. Dev Dyn. 2006; 235:2470–2482. [PubMed: 16691564]

Peters K, Ornitz D, Werner S, Williams L. Unique expression pattern of the FGF receptor 3 gene during mouse organogenesis. Dev Biol. 1993; 155:423–430. [PubMed: 8432397]

Pirvola U, Cao Y, Oellig C, Suoqiang Z, Pettersson RF, Ylikoski J. The site of action of neuronal acidic fibroblast growth factor is the organ of Corti of the rat cochlea. Proc Natl Acad Sci U S A. 1995; 92:9269–9273. [PubMed: 7568115]

Pirvola U, Ylikoski J, Trokovic R, Hebert JM, McConnell SK, Partanen J. FGFR1 is required for the development of the auditory sensory epithelium. Neuron. 2002; 35:671–680. [PubMed: 12194867]

Pujades C, Kamaid A, Alsina B, Giraldez F. BMP-signaling regulates the generation of hair-cells. Dev Biol. 2006; 292:55–67. [PubMed: 16458882]

Rubel EW, Fritzsch B. Auditory system development: primary auditory neurons and their targets. Annu Rev Neurosci. 2002; 25:51–101. [PubMed: 12052904]

Shim K, Minowada G, Coling DE, Martin GR. Sprouty2, a mouse deafness gene, regulates cell fate decisions in the auditory sensory epithelium by antagonizing FGF signaling. Dev Cell. 2005; 8:553–564. [PubMed: 15809037]

Sobkowicz HM, Emmerling MR. Development of acetylcholinesterase-positive neuronal pathways in the cochlea of the mouse. J Neurocytol. 1989; 18:209–224. [PubMed: 2732759]

Woods C, Montcouquiol M, Kelley MW. Math1 regulates development of the sensory epithelium in the mammalian cochlea. Nat Neurosci. 2004; 7:1310–1318. [PubMed: 15543141]

Xiang M, Gao WQ, Hasson T, Shin JJ. Requirement for Brn-3c in maturation and survival, but not in fate determination of inner ear hair cells. Development. 1998; 125:3935–3946. [PubMed: 9735355]

Zhang X, Ibrahimi OA, Olsen SK, Umemori H, Mohammadi M, Ornitz DM. Receptor specificity of the fibro-blast growth factor family. The complete mammalian FGF family. J Biol Chem. 2006; 281:15694–15700. [PubMed: 16597617]

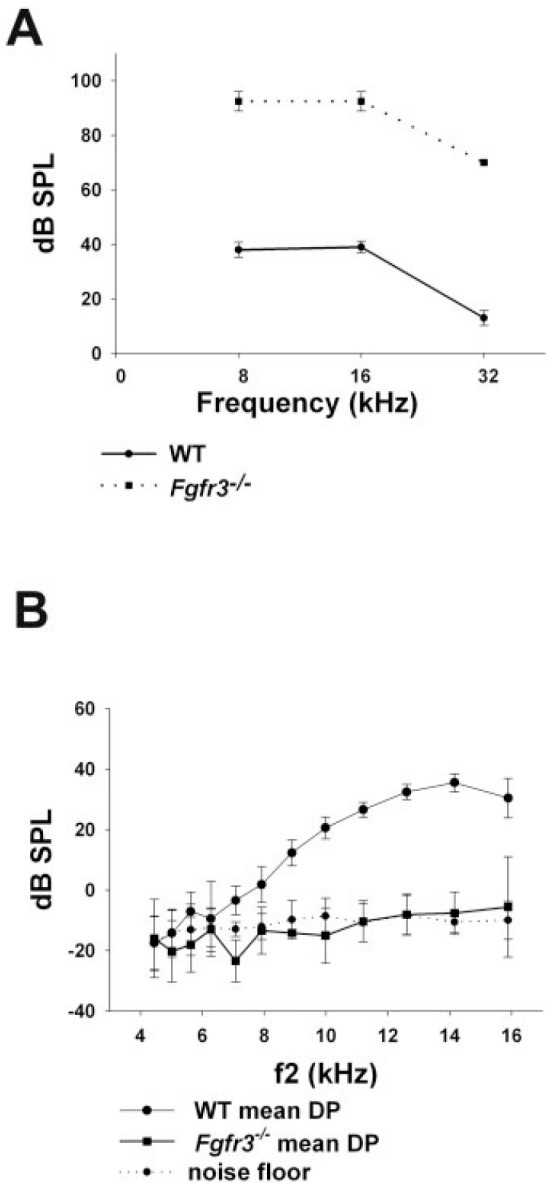

Fig. 1.

Auditory deficits in *Fgfr3*$^{-/-}$ mice. **A:** Auditory brainstem response (ABR) thresholds from 3-month-old *Fgfr3*$^{-/-}$ and wild-type (WT) littermate controls. Vertical bars indicate standard deviations. A shift of approximately 50 dB was observed at all frequencies tested. **B:** Mean distortion product otoacoustic emission (DPOAE) amplitudes for both ears of a representative *Fgfr3*$^{-/-}$ mouse and a WT littermate at 3 months of age. The recorded amplitudes for the mutant are indistinguishable from the noise floor (background). Vertical bars indicate standard deviation. DP, distortion product.

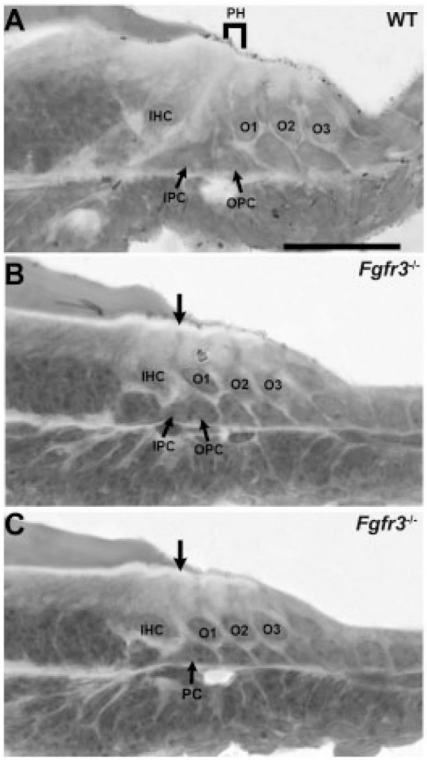

Fig. 2.

Cellular patterning is disrupted in *Fgfr3*$^{-/-}$ cochleae. Mid-modiolar cross-sections of postnatal day (P) 0 cochlea from wild-type (WT) and *Fgfr3*$^{-/-}$ mice. **A:** In the mid-basal turn of a WT cochlea, the nuclei for the inner pillar cell (IPC) and outer pillar cell (OPC) are present in the region between the inner hair cell (IHC) and first outer hair cell (OHC, O1). Projections from IPC and OPC extend to the luminal surface to generate the developing pillar head (PH). **B:** The basal turn in an *Fgfr3*$^{-/-}$ cochlea contains two cell nuclei (IPC and OPC) between IHC and O1. However, the luminal projections that give rise to the developing pillar head are disrupted (arrow). **C:** In a more apical section from the same cochlea as in B, only a single nucleus (PC) is present in the region between IHC and O1 and no pillar head extends to the luminal surface (arrow). Scale bar = 50 μm in A (applies to B,C).

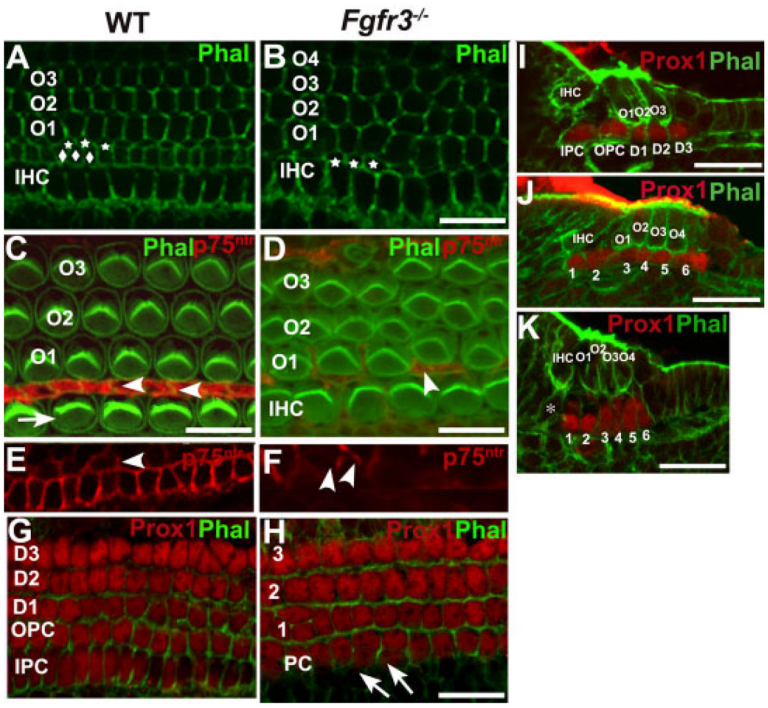

Fig. 3.

Pillar cells are absent in *Fgfr3*$^{-/-}$ cochleae. **A,B:** Luminal surface of the organ of Corti from wild-type (WT) and *Fgfr3*$^{-/-}$ cochleae at postnatal day (P) 0. Cortical actin filaments are labeled with phalloidin. In WT, the pillar head located between the row of inner hair cells (IHCs) and O1s, is composed of a row of cuboidal inner pillar cell (IPC) projections (diamonds) and a row of diamond-shaped outer pillar cell (OPC) projections (stars). In contrast, in *Fgfr3*$^{-/-}$ mutants only a single row of diamond-shaped pillar heads are present (stars). IHC, inner hair cells; O1–O3, outer hair cell (OHC) O1–O3. C–F: p75^{ntr} labeling is shown in red (C–F) and phalloidin labeling in green (C,D) in the organ of Corti at P0. **C:** In a WT cochlea, p75^{ntr} is strongly expressed in the cuboidal IPCs (arrowheads) present between the row of IHCs and O1s. **E:** In addition, the interdigitations of OPCs between O1 cells are also evident (arrowhead). **D,F:** In contrast, in *Fgfr3*$^{-/-}$ cochlea, the cuboidal row of p75^{ntr}-positive IPCs is absent, although p75^{ntr}-positive interdigitations still persist between O1 cells (arrowheads). D: p75^{ntr} also labels Hensen's cells located lateral to the third row of OHCs in both WT (not shown) and *Fgfr3*$^{-/-}$ cochleae (D). **G,H:** Whole-mount view of Prox1-positive nuclei (red) in the basal turn of WT and *Fgfr3*$^{-/-}$ cochleae at P0. Cell boundaries are labeled with phalloidin (green). In WT, a single row of oblong IPC nuclei is located adjacent to four rows (OPC + D1–3) of cuboidal nuclei. In contrast, in the *Fgfr3*$^{-/-}$ cochlea, the row of oblong nuclei is absent and four or five (arrows) of cuboidal nuclei are present. The images in G and H have been aligned based on the position of overlying hair cells (not shown). PC, pillar cell nuclei; D1–3, Deiters' cell nuclei. **I:** Cross-section through the organ of Corti in the basal turn of a WT at P0, illustrating the positions of Prox1-positive cells. The inner and outer pillar cell nuclei, IPC, and OPC, respectively, are located in the region between IHC and O1 and are positive for Prox1. In addition, the three Deiters' cells (D1–3) are also positive for Prox1. **J,K:** Cross-sections through the basal turn of the organ of Corti of an *Fgfr3*$^{-/-}$ cochlea at P0. In J, although the differentiation of the pillar cells is disrupted, two Prox1-positive cells (1 and 2) are located in the region between IHC and O1. Four other Prox1-positive cells (3– 6) are located beneath the OHCs (O1– 4), suggesting that these are Deiters' cells. In contrast, in K, only a single Prox1-positive cell is located between

IHC and O1 (1), while five Prox1-positive cells (2–5) are located beneath the OHCs (O1–3). However, it should be noted that Prox1-postive cell 4 appears to be a fragment of a cell and probably represents a Prox1-positive cell located adjacent to either cell 3 or 5. An additional Prox1-negative cell (asterisk) might represent a cell that has moved into the pillar cell space in response to changes in pillar cell development. Scale bars = 20 μm in A–K.

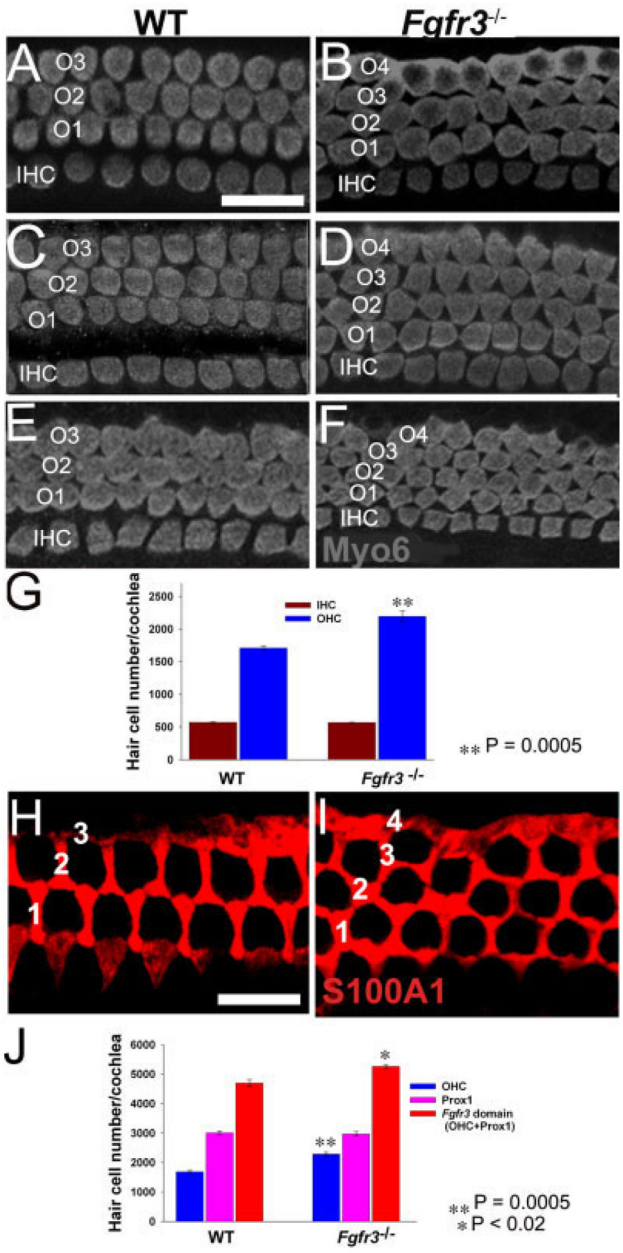

Fig. 4.

Additional outer hair cells (OHCs) and Deiters' cells are present in *Fgfr3*$^{-/-}$ cochleae. **A,C,E:** Surface views of the organ of Corti from the basal (A), middle (C), and apical (E) turns of the cochlea from a wild-type (WT) mouse at postnatal day (P) 0. Anti-Myosin6 labeling indicates a single row of inner hair cells (IHC) and three rows of OHCs (O1–3) present along the length of the cochlea. **B,D,F:** Comparable views to those illustrated in A,C,E from an *Fgfr3*$^{-/-}$ cochlea. A fourth row of OHCs (O4) begins at approximately the 40% position along the basal-to-apical axis and continues to the apex. **G:** Quantification of the total number of IHCs and OHCs in cochleae from *Fgfr3*$^{-/-}$ and WT littermates showed a significant increase in the number of OHCs (n = 3; $P = 0.0005$). Error bars are SEM. **H,I:** Analysis of Deiters' cells labeled with anti-S100A1 in WT (H) and *Fgfr3*$^{-/-}$ mutants (I) at P8 indicates the presence of an ectopic row of Deiters' cells in *Fgfr3*$^{-/-}$ cochleae. 1– 4: Four

rows of Deiters' cells. **J:** Quantification of total number of Prox1-positive cells and total cells in the pillar cell/OHC region indicates that, while there is no change in the number of Prox1-positive cells, there is a significant increase in total cells in the pillar cell/OHC region (n = 3; $P = 0.02$) as a result of the increase in OHCs ($P < 0.0005$). Scale bar = 20 μm in A–F, 20 μm in H,I.

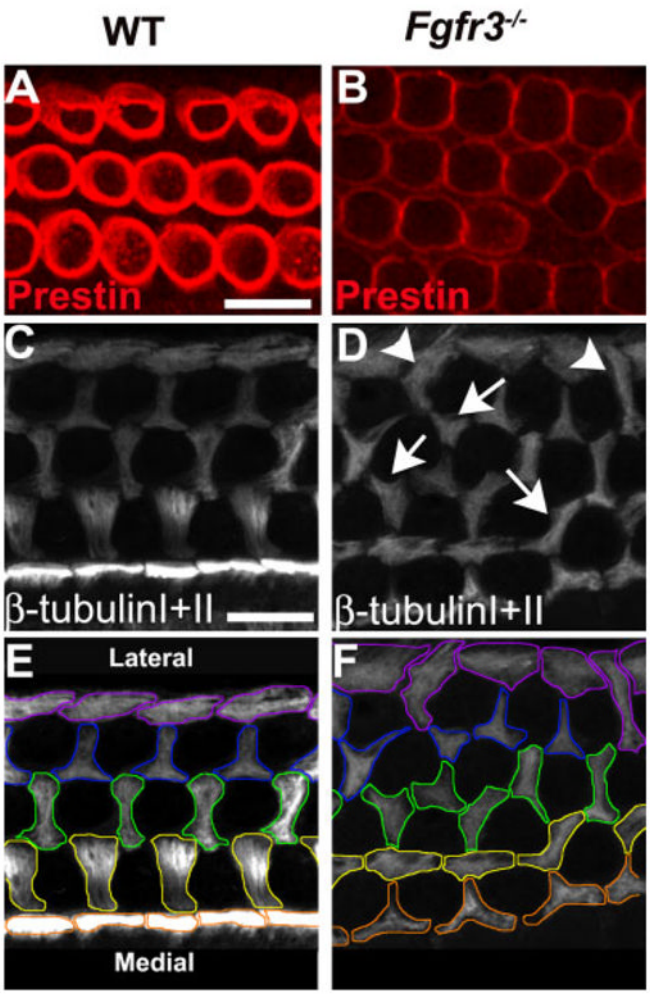

Fig. 5.

Differentiation of outer hair cells (OHCs) and Deiters' cells is disrupted in *Fgfr3*$^{-/-}$ cochleae. **A,B:** Expression of Prestin in OHCs. Wild-type (WT) and *Fgfr3*$^{-/-}$ littermates were imaged on a confocal microscope using the same intensity and sensitivity settings. The level of Prestin appears to be lower in the four rows of OHCs in the *Fgfr3*$^{-/-}$ cochlea. **C–F:** Anti-β-tubulin I + II staining was used to label microtubules at the luminal surface in pillar cells and Deiters' cells in WT (C,E) and *Fgfr3*$^{-/-}$ cochleae (D,F). In E and F, luminal microtubules have been outlined in colors corresponding to their relative position in the epithelium. In WT, microtubule bundles in inner pillar heads (orange in F) have a rectangular shape and form a continuous row. Microtubule bundles in outer pillar heads (yellow outline in F) and in the first-row (green outline) and second-row (blue outline) Deiters' cells are oriented along the mediolateral axis and have stereotypical morphologies. Third-row Deiters' cells form a row of boundary cells (purple) that do not form interdigitations between hair cells. D,F: In contrast with WT, the orientations of both pillar cells and Deiters' cells is disrupted in *Fgfr3*$^{-/-}$ cochleae. D: In particular, there are examples of cells with microtubule bundles that branch in multiple directions (arrows). D: Similarly, there are examples of third-row Deiters cells that project medially directed microtubules to form interdigitations between fourth row OHCs (arrowheads). The colored outlines in F illustrate the marked changes in the morphologies of Deiters' cells in all rows of the organ of Corti. Scale bar = 20 μm in A,B, 10μm in C–F.

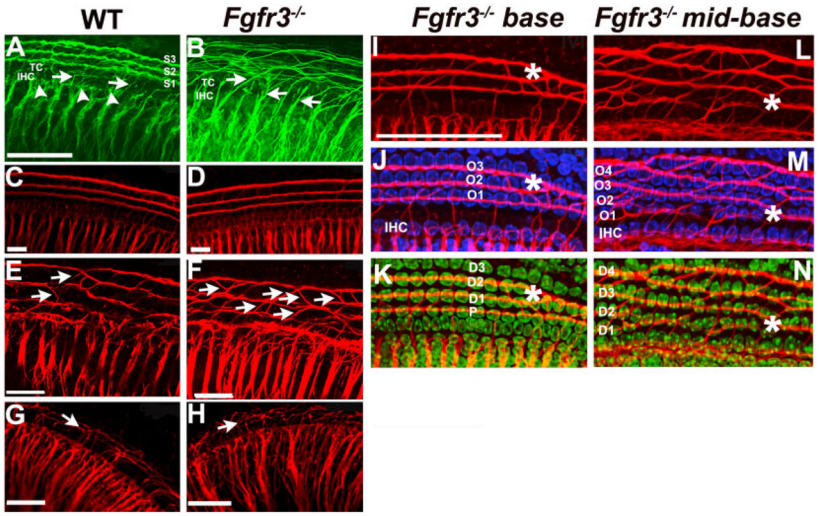

Fig. 6.

Innervation is disrupted in *Fgfr3*$^{-/-}$ cochleae. **A,B:** Anti-neurofilament staining of afferent and efferent neurons in postnatal day (P) 8 cochlea from the mid-basal turn of wild-type (WT, A) and *Fgfr3*$^{-/-}$ (B) mice. In WT, most fibers appear to terminate in the inner hair cell region (IHC, arrowheads) with a limited number crossing the tunnel of Corti (TC, arrows). After crossing the tunnel, spiral fibers (S1–3) turn toward the base (the right side of the image) to form synapses on outer hair cells (OHCs). In contrast, in *Fgfr3*$^{-/-}$ cochleae, a greater number of fibers cross the tunnel of Corti (arrows) and once in the OHC region, these fibers do not coalesce to form discrete fiber bundles. **C–H:** DiI (1,1′, di-octadecyl-3,3,3′,3′,-tetramethylindo-carbocyanine perchlorate) -labeling of afferent neurons in P1 cochleae from WT (C,E,G) and *Fgfr3*$^{-/-}$ (D,F,H) mice; the basal (C,D), middle (E,F), and apical regions (G,H) of the cochlea are illustrated. F,H: As observed with neurofilament staining, the pattern of afferent innervation is disrupted in the middle and apical turns of the *Fgfr3*$^{-/-}$ cochlea. In particular, the number of crossing fibers (arrows) between the rows of spiral fibers is increased. C,D: In contrast, the innervation pattern appears relatively normal in the base. **I–N:** Tubulin staining of nerve fibers (I,L) and combined nerve fiber stain with Hoechst labeling of nuclei (J,K,M,N) of basal (I,J,K) and of mid-basal turns (L,M,N) from an *Fgfr3*$^{-/-}$ cochlea. Nerve fibers represent a collapse of a stack through the entire cochlea. J,K,M,N: Hoechst stain represents single confocal optical sections at the level of hair cells (J,M) or supporting cells (K,N). Images are aligned based on fiber staining. J: In the less affected base, fibers extend laterally across the pillar cell space before turning to form outer spiral bundles that correlate with the three rows of hair cells (O1–O3). K: At the supporting cell level, the position of fiber turning correlates with the lateral edge of the second row of pillar cells. J,K: At the position indicated by the asterisk, the number of rows of OHCs (J) and Deiters' cells (K) changes from three to two. Note that the spiral fibers converge as well. M: In the more affected mid-basal region, IHCs and OHCs are considerably closer together. The region of lateral fiber extension is lost and some fibers begin to turn as soon as they pass the IHCs. M,N: In addition, the rows of both OHCs (M) and supporting cells (N) are noticeably disorganized. In some cases, disorganization in the arrangement of supporting cell rows correlates with the presence of fibers crossing between spiral bundles (asterisk), suggesting that the defects in patterning of supporting cells may contribute to defects in innervation. Scale bars = 20 μm in A (applies to B), 10 μm in C,D, 20 μm in E–H, 50 μm in I,L–N.

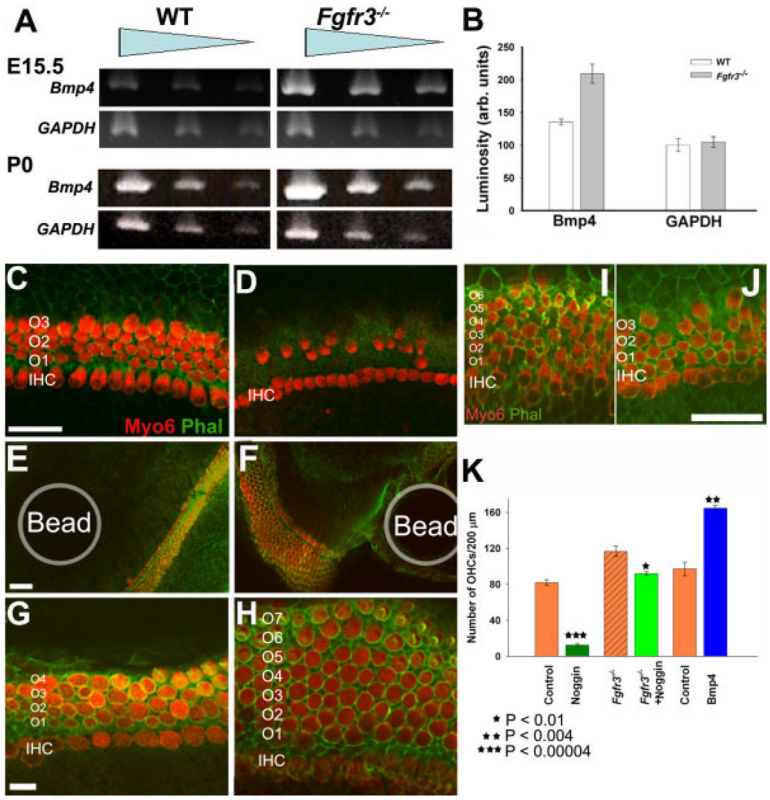

Fig. 7.

Bmp4 is negatively regulated by fibroblast growth factor receptor 3 (FGFR3). **A:** Semiquantitative polymerase chain reaction amplification for *Bmp4* from total RNA isolated from wild-type (WT) and $Fgfr3^{-/-}$ littermates at embryonic day (E) 15.5 and postnatal day (P) 0 indicates an increase in the mRNA level of *Bmp4* in cochleae from $Fgfr3^{-/-}$ mice at both ages. For both WT and $Fgfr3^{-/-}$ cochleae, the starting concentration of template cDNA was diluted by 1/3 between lanes 1 and 2 and by 1/3 again between lanes 2 and 3. **B:** Quantification of levels of *Bmp4* from WT and $Fgfr3^{-/-}$ cochleae at E15.5 as determined by measuring the level of incorporation of ethidium bromide (see the Experimental Procedures section for further details). There is a clear increase in the level of *Bmp4* in cochleae from $Fgfr3^{-/-}$ mice. The mRNA for *GAPDH* served as a loading control. n = 2, and error bars are SEM. C,D: Noggin inhibits hair cell development. **C:** Sensory epithelium in a control explant in which hair cells have been labeled with Myosin6 (red) and cell boundaries have been labeled with phalloidin (green). A single row of inner hair cells (IHCs) and four rows of outer hair cells (OHCs, O1–O4) are present. **D:** Sensory epithelium from an explant treated with Noggin (5 μg/ml) beginning on E15.5 and labeled as in C. IHCs appear normal, but the number and patterning of OHCsis significantly disrupted. E–H: Bone morphogenetic protein 4 (BMP4) induces OHC formation. **E:** Low-magnification image of a cochlear explant containing a phosphate buffered saline (PBS) -soaked control bead (Bead) introduced on E15.5 and labeled as in C. The development of the sensory epithelium is unaffected by the presence of the bead. **F:** Low-magnification image of cochlear explant culture containing a bead soaked in 40 μg/ml recombinant BMP4 protein (Bead) beginning on E15.5. There is a marked increase in the number of OHCs in the sensory epithelium located near the bead. **G:** High-magnification image of the sensory epithelium in a cochlear explant culture containing a control bead. The pictured region was located within 200 μm of the bead. Note the three to four rows of OHCs (O1–O4) and one row of IHCs. **H:** High-

magnification image of the same cochlear explant culture as in H containing a bead soaked with recombinant BMP4 protein. A single row of IHCs is present, but the number of rows of OHCs has increased to between seven and nine. I–J: Extra OHCs in *Fgfr3*$^{-/-}$ mutants are inhibited by Noggin. **I:** Sensory epithelium from the basal region of an explant established from an *Fgfr3*$^{-/-}$ mutant at E13.0. Several additional rows of OHCs (numbered) are present. **J:** Sensory epithelium from an *Fgfr3*$^{-/-}$ explant as in I, but maintained in the presence of 3 μg/ml Noggin beginning after 2.5 days in vitro. The rows of OHCs are reduced to three. **K:** Quantification of the change in density of OHCs in control or *Fgfr3*$^{-/-}$ explants exposed to Noggin or containing BMP4-coated beads. Treatment of control explants with Noggin resulted in significant reduction in the number of OHCs (n = 3; $P = 0.00004$), while IHCs were unchanged (not shown). An increase in the number of OHCs was observed in explants from *Fgfr3*$^{-/-}$ mutants; however, this increase was eliminated in the presence of Noggin (n = 3, $P < 0.01$). In contrast, there was a significant increase in the number of OHCs in regions of the sensory epithelium located within 100 μm of a BMP4-coated bead (n = 3; $P < 0.004$). The control data for the BMP4 experiment represents the number of hair cells within 100 μm of a PBS-coated bead. Scale bars μ 20 μm in C (applies to D), 50 μm in E (applies to F), 20 μm in G (applies to H,I,J).